

# Enhancement of Luminescence Intensity in Dy<sup>3+</sup> Ions Doped YVO<sub>4</sub> Nanomaterials by Ba<sup>2+</sup> Ion Codoping and YVO<sub>4</sub>:2Dy/Fe<sub>3</sub>O<sub>4</sub> Nanohybrid for Hyperthermia Application

Laishram Priyobarta S<sup>1</sup>, Ningthoujam Premananda S<sup>2</sup> and Thiyam David S<sup>1\*</sup>

<sup>1</sup>National Institute of Technology, Imphal-795004, India

<sup>2</sup>Department of Chemistry, Manipur University, Imphal-795003, India

## Abstract

The enhancement of the luminescence intensity of the Dy<sup>3+</sup> by Ba<sup>2+</sup> ions (at different concentrations) codoping into YVO<sub>4</sub>:2Dy nanoparticles at different annealing temperature of as-prepared, at 500 and 900°C were studied. The XRD study shows the strains are induced when dopant and codopant are incorporated into host matrix. XRD patterns of nanohybrids show the existence of two phases corresponding to YVO<sub>4</sub>:2Dy and Fe<sub>3</sub>O<sub>4</sub> nanoparticles. TEM image of YVO<sub>4</sub>:2Dy nanoparticles were spherical shape whereas for YVO<sub>4</sub>:2Dy/Fe<sub>3</sub>O<sub>4</sub> nanohybrids, the spherical particles are forming chain like structure due to the PEG molecule which binds both YVO<sub>4</sub>:2Dy and Fe<sub>3</sub>O<sub>4</sub> during nanohybrids formation. Increase in absorption coefficient and decrease in lattice strain values are the major reasons for the enhancement of emission intensity in photoluminescent (PL). Lifetime studies also shows correlation between the calculated energy transfer and diffusion for indirect excitation which is also studied here. High quantum efficiency up to 45% can be achieved. YVO<sub>4</sub>:2Dy/Fe<sub>3</sub>O<sub>4</sub> nanohybrids is found to achieve hyperthermia temperature 42°C in short time. This nanohybrids shows luminescence in the region of biological window indicating nanohybrids can be used as bioimaging probe. It also shows high viability up to 94% in HeLa cancer cells.

**Keywords:** Vanadate nanoparticles; Enhancement of luminescence; Nanohybrids; Hyperthermia; HeLa cell

## Introduction

Lanthanide (rare-earth (RE)) doped phosphor materials have wide applications, including phosphors, display device, bio-imaging, scintillators, and amplifiers for fiber-optic communications [1-3]. Amongst the phosphor materials YVO<sub>4</sub> is one of the excellent host lattice for lanthanide ions which producing variety of colors photoluminescence. It can be used as an excellent polarizer and laser host material also. YVO<sub>4</sub> doped with lanthanide have been used as attractive phosphor because of its high luminescence quantum yield. In YVO<sub>4</sub>, there are two ways of efficient energy transfer to lanthanide, one is RE-O and other is VO<sub>4</sub><sup>3-</sup> to RE [4]. In previous report powder YVO<sub>4</sub>:Eu show high luminescence quantum yield of about 70% under ultraviolet (UV) excitation [5] and moreover in the colloids state also YVO<sub>4</sub>:Eu nanoparticles (NPs) also show high quantum yield and better brightness in comparison with the other RE-doped nanophosphors [6].

In order to minimize the agglomeration of NPs, long chain organic molecules are used as capping agents [7]. In this work ethylene glycol (EG) is used both as capping agent and solvent medium. EG is non-toxic and can be easily washed with water, methanol, ethanol, acetone, etc. Due to presence of polar functional group, NPs capped with EG are water dispersible and such water dispersibility properties makes them applicable in biolabelling through optical imaging [8].

Improvement of luminescence intensity is important in luminescence studies. Amongst the various methods to improve the luminescence intensity of the lanthanides. Co-doping one of the choices to improved luminescence intensity.

In this work we have prepared YVO<sub>4</sub> nanoparticles doped with Dy<sup>3+</sup> ion (at different concentration) and YVO<sub>4</sub>:2Dy co-doped with Ba<sup>2+</sup> ion (at different concentration of Ba<sup>2+</sup> ions) by polyol method. The samples are annealed at 500 and 900°C and studied its luminescence properties, lifetime and quantum yield. In lifetime study, nonlinear curve fitting have been used to study diffusion (D) and energy transfer process in

case of indirect excitation of Dy<sup>3+</sup> ion, which was not studied in many previous reports. We also prepared YVO<sub>4</sub>:2Dy/Fe<sub>3</sub>O<sub>4</sub> nanohybrid and studies its hyperthermia under AC magnetic field. We found that the prepared nanohybrid can achieved hyperthermia temperature (42°C) in a short period. This hybrid material can be used for hyperthermia application in cancer therapy.

## Experimental Section

### Reagents and materials

Yttrium nitrate hexahydrate, (Y(NO<sub>3</sub>)<sub>3</sub>.6H<sub>2</sub>O (99.99%)), dysprosium nitrate hydrate (Dy(NO<sub>3</sub>)<sub>3</sub>.xH<sub>2</sub>O, 99.99%) and ammonium metavanadate (NH<sub>3</sub>VO<sub>3</sub>, 99.99%) from Alfa Aesar, ethylene glycol and ammonia solution from Merck and methanol were used as received. The whole experiment was carried out using double distilled water.

### Synthesis of YVO<sub>4</sub>:Dy<sup>3+</sup> nanoparticles

0.02, 0.05 and 0.07 of Dy<sup>3+</sup> ion doped YVO<sub>4</sub> nanoparticles were synthesized by ethylene glycol route. For the preparation of 2 at.% Dy<sup>3+</sup> ion doping concentration, 0.0377 g of Dy(NO<sub>3</sub>)<sub>3</sub>.6H<sub>2</sub>O and 1.671 g of Y(NO<sub>3</sub>)<sub>3</sub>.6H<sub>2</sub>O were taken and dissolved in 10 mL water. Further, 50 mL of ethylene glycol were added and heated in a round bottom flask at 40°C for 30 minutes. 1 g of ammonium metavanadate was added and it was allowed to reflux at 40°C for 30 minutes. Then 5 mL of ammonia

**\*Corresponding author:** Thiyam David Singh, Department of Chemistry, National Institute of Technology, Manipur, India, Tel: 913852413031; E-mail: davidthiyam@gmail.com

Received June 08, 2017; Accepted June 20, 2017; Published June 26, 2017

**Citation:** Laishram Priyobarta S, Ningthoujam Premananda S, Thiyam David S (2017) Enhancement of Luminescence Intensity in Dy<sup>3+</sup> Ions Doped YVO<sub>4</sub> Nanomaterials by Ba<sup>2+</sup> Ion Codoping and YVO<sub>4</sub>:2Dy/Fe<sub>3</sub>O<sub>4</sub> Nanohybrid for Hyperthermia Application. J Nanomed Nanotechnol 8: 445. doi: 10.4172/2157-7439.1000445

**Copyright:** © 2016 Laishram Priyobarta S, et al. This is an open-access article distributed under the terms of the Creative Commons Attribution License, which permits unrestricted use, distribution, and reproduction in any medium, provided the original author and source are credited.

solution was added and refluxed at 160°C for 2 h. The resulting white precipitate was collected after repeated washing with methanol by centrifugation at 10000 rpm. The precipitate was annealed at different temperatures 500 and 900°C for 2 h each.

### Synthesis of 1 at.% Ba codoped in YVO<sub>4</sub>:2Dy Nanoparticles

1 at.% Ba codoped in YVO<sub>4</sub>:2Dy nanoparticles were synthesized using same procedure as above. Here, 0.0377 g of Dy(NO<sub>3</sub>)<sub>3</sub>·6H<sub>2</sub>O, 0.0112 g of BaNO<sub>3</sub> and 1.60 g of Y(NO<sub>3</sub>)<sub>3</sub>·6H<sub>2</sub>O were dissolved in 10 mL water and then 50 mL of ethylene glycol is added. The solution is heated in a round bottom flask at 40°C for 30 minutes. 1 g of ammonium metavanadate was added and refluxed at 40°C for 30 minutes. Same amount of ammonia solution was added and refluxed at 160°C for 2 h. The precipitate thus formed is collected by centrifugation and kept it for annealing at two different temperatures same as mentioned above for Dy doping. Similar procedures were also carried out for the other concentrations of Ba<sup>2+</sup> ion codoping by taking required stoichiometric amount.

### Synthesis of hybrid nanoparticles

Hybrid nanoparticles YVO<sub>4</sub>:2Dy/Fe<sub>3</sub>O<sub>4</sub> were prepared using 4:1 wt.% ratio of YVO<sub>4</sub>:2Dy and Fe<sub>3</sub>O<sub>4</sub> i.e. 2, 4 and 6 mg of Fe<sub>3</sub>O<sub>4</sub> were thoroughly ground with 8, 16 and 24 mg of YVO<sub>4</sub>:2Dy, respectively. Each mixture was sonicated for 30 min in 1 mL of PEG (polyethylene glycol) solution in order to get highly dispersed hybrid nanomaterials. Moreover, PEG solution using here was prepared after dissolution of 100 mg of 6000 PEG solute in 100 mL of distilled water). Detailed studies of preparation of Fe<sub>3</sub>O<sub>4</sub> using Fe<sup>2+</sup> and Fe<sup>3+</sup> precursor with subsequent hydrolysis by NH<sub>4</sub>OH and its magnetisation studies were reported elsewhere [9].

### Cell culture

For in-vitro cytotoxicity study, all experiments were performed on HeLa (Human Negroid cervix Epitheloid Carcinoma) cell lines which were received from the National Centre for Cell Sciences, Pune, India. To perform the detailed toxicity study, HeLa cells were allowed to grow in MEM + 10% FBS + antibiotics at temperature 37°C in 5% CO<sub>2</sub> atmosphere and using MTT assay technique. The testing was carried out by the National Toxicology Centre, Pune, India.

### MTT assay

In a 96-well microtiter plate, at a concentration of 2 × 10<sup>5</sup> cells μL<sup>-1</sup>, the cells were incubated for 24 h in appropriate medium. Old media was replaced again by fresh media after 24 h having sets of different concentration of sterilized magnetic nanoparticles YVO<sub>4</sub>:2Dy/Fe<sub>3</sub>O<sub>4</sub> (0.2, 0.4, 0.6 and 0.8 μg / mL cultured media). The whole medium was again incubated for 24 h at 37°C in a 5% CO<sub>2</sub> atmosphere. The incubated microtiter plates were observed periodically under inverted microscope for coloured precipitate and other parameters. Then, 10 mL MTT solution was added into each wells. After incubated for 3 h in same conditions for metabolization of MTT with the nanoparticles and cell media. The total medium was then removed from the plates and the cells were washed with PBS. The formazan thus formed was dissolved and extracted using 200 mL acidic iso-propanol. Absorbance measurement is carried out at 570 nm of control and experimental well to calculate cell viability. To overcome errors, the experiments were done three times and average absorbance vs cell density is plotted for further calculation of viability.

### Characterization

Philips x-ray diffractometer (PW 1071) having x-ray radiation generated from CuK<sub>α</sub> (1.5405 Å) with Ni filter was used to measure diffraction patterns. The corresponding angular range 10 ≤ 2θ/deg ≤ 80 with a step size of Δ2θ = 0.02 was used during measurements. A thick layer of ground powder sample were dispersed on a glass slide using methanol and allowed it to dry for some time. Scherrer relation is used to calculate the average crystallite size (*t*) of sample which is given as  $t = 0.9\lambda/\beta \cos \theta$  where λ is the wavelength of the x-ray i.e. 1.54 nm and β is the full width at half maximum (FWHM). The lattice parameters a, b, c was calculated using least square fitting from diffraction peaks.

FTIR spectra were recorded using Perkin Elmer Spectrum 400 FT-IR Spectrometer. Thin pellets of sample mixed with KBr were made and kept in sample holder under IR irradiation.

TEM images were captured using JEOL 2000 FX transmission electron microscope. The powder samples were sonicated to disperse in methanol. With the help of a micropipette a fine drop containing dispersed nanoparticles is put in copper grid.

Luminescence measurements of YVO<sub>4</sub>:Dy nanoparticles were carried using Edinburgh Instrument FLS920 having μs-flash lamp. A thin layer of powdered samples was pasted on glass slide using methanol and dried in oven to evaporate methanol. The quantum yield measurement was also carried out using Edinburgh Instrument FLS920 installed with integrated sphere. A quartz cuvette containing 10 mg of sample which was dispersed in 10 ml of Methanol (solvent) is place in sample holder and excited with excitation wavelength 320 nm. The number of photons absorbed (α) by sample was measured as emission scan for  $I_{solvent}$  or  $I_{sample}$  from 300 nm to 340 nm so as the excitation wavelength can be seen in the form of emission spectrum. Difference between areas under curve of  $I_{solvent}$  and  $I_{sample}$  will give the number of photons absorbed. Similarly, emission scan for  $I_{emission}$  is also recorded from 565-585 nm to get emission spectrum of sample.

Generation of heat from the sample was studied with the help of Easy Heat 8310 instrument, Ambrell, UK. Induction coil contains 4 turns with approximate diameter of the coil 6 cm. Fixed frequency at 265 kHz is now applied to the sample. The whole experiment set up is dipped into a normal water circulation to maintain constant temperature throughout. 2-6 mg of samples dispersed in 1 mL PEG solution is put in a 1.5 mL micro centrifuge tube and kept at the centre of the coil where maximum magnetic is felt. Heating of the sample with variable current at 200, 300 and 400 A up to 10 min is performed for every sample. An optical temperature sensor (Photon R & D, Canada) with accuracy of ±0.01°C is used to record temperature while keeping it in contact with sample inside the medium.

Magnetic field generated with different currents applied is given by

$$H = \frac{1.257ni}{L}$$

Where H signifies magnetic field experience by sample, n is the number of turns of induction coil, i is the current applied and diameter of turn in cm is denoted as L. The various calculated values of the magnetic fields w.r.t. Currents 200, 300 and 400 A was found to be 168, 251 and 335 Oe which is equivalent to 13, 20 and 27 in kA m<sup>-1</sup> unit.

## Result and Discussion

### X-ray Diffraction study

Figure 1A shows the X-ray diffraction pattern of YVO<sub>4</sub>:2Dy as-prepared and at different annealing temperature of 500 and 900°C. All peak patterns can be related to well crystalline having tetragonal phase with space group I4<sub>1</sub>/amd (141). Different planes are assigned to corresponding peaks and it is shown here. Similar peak patterns can be observed for 3 at.% co-doped Ba<sup>2+</sup> ion codoped YVO<sub>4</sub>:2Dy also (Figure 1B). The as-prepared samples show low crystallinity as indicated by low sharpness of peaks, and as the annealing temperature raise the crystallinity of the samples also increases which is observed with sharp peaks.

The full widths half maximum (FWHM) values for YVO<sub>4</sub>:2Dy are found as 0.2513, 0.2626 and 0.2445°, respectively in 2θ scale for as-prepared, 500 and 900°C annealed samples. For YVO<sub>4</sub>:2Dy:3Ba, FWHM values are 0.2670, 0.3156 and 0.2402°, respectively for as-prepared, 500 and 900°C annealed samples. The lattice parameter and crystallite size are given in Table 1. Decrease in crystallite size for 500°C annealed sample as compared to as-prepared sample is due to incorporation of impurities C (carbon) left after decomposition of ethylene glycol [3].

To study the microstrain induced by dopant and codopant ions, we have employed Williamson-Hall model [10] which is

$$\beta \cos\theta = 0.9\lambda/D + 4\epsilon \sin\theta$$

Here, β is the FWHM at Bragg's angle (2θ), is the X-ray wavelength i.e. 1.54 Å. D is treated as effective crystallite size. As observed from

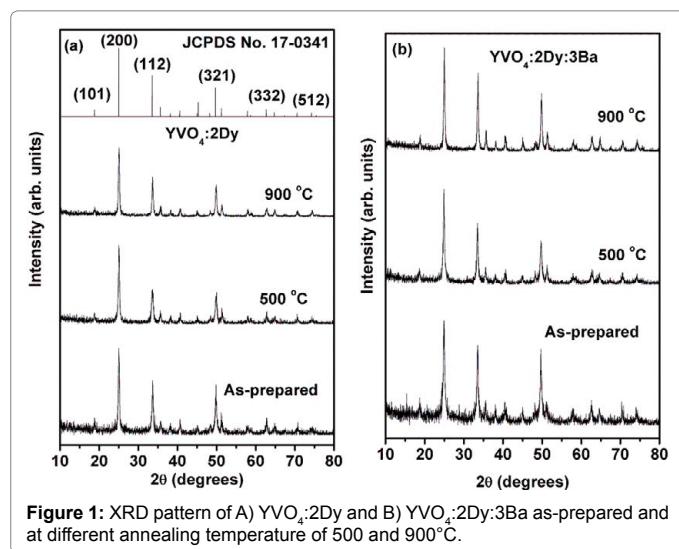
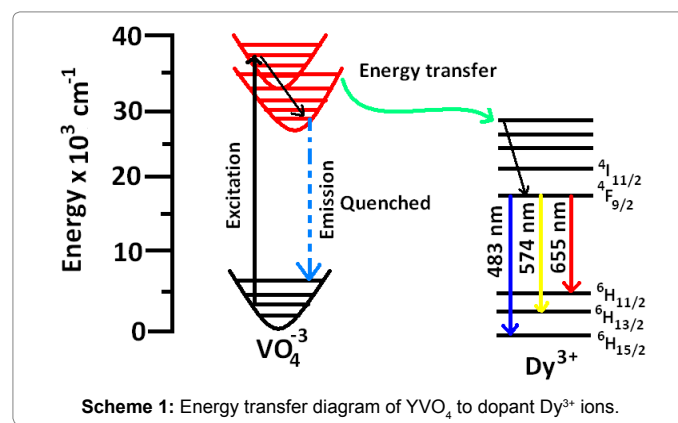


Table 1 strain values can be tuned with doping of Dy<sup>3+</sup> and Ba<sup>2+</sup> ion the i.e. Strain value of Dy<sup>3+</sup> ion doped YVO<sub>4</sub> (-0.122%) is suddenly drop when codoped with 2 at.% Ba<sup>2+</sup> ion is (-0.098%) for 900°C annealed samples. The positive strain indicates tensile strain and negative strain value corresponds to compressive strain. A similar decrease in tensile strain value is also seen for Ba<sup>2+</sup> ion codoped YVO<sub>4</sub> nanoparticles at other annealing temperature.

In case of YVO<sub>4</sub>:2Dy/Fe<sub>3</sub>O<sub>4</sub> nanohybrids the XRD patterns show both phase of YVO<sub>4</sub> and Fe<sub>3</sub>O<sub>4</sub> nanoparticles which is shown in Supplementary Figure S1. For Fe<sub>3</sub>O<sub>4</sub> phase the peaks pattern can be indexed with JCPDS no. 85-1436 having cubical phase with space group Fd3m (227). Here, the peaks of Fe<sub>3</sub>O<sub>4</sub> are too small compared to the YVO<sub>4</sub> due to its small quantity (1:4). Moreover, most of the intense peaks of Fe<sub>3</sub>O<sub>4</sub> are coincided with peaks originated from YVO<sub>4</sub> and due to this effect even some small peaks of YVO<sub>4</sub> seems more intense when they formed hybrid with Fe<sub>3</sub>O<sub>4</sub>. The star mark in the Supplementary Figure S1 indicates the Fe<sub>3</sub>O<sub>4</sub> phase.

### Vibrational study

Figure 2 shows the FTIR spectra of as prepared, 500 and 900°C annealed samples of YVO<sub>4</sub>:2Dy nanoparticles. The peak at 815 cm<sup>-1</sup> can be assigned to the V-O stretching vibration originated from VO<sub>4</sub> tetrahedron and the band around at 300-436 cm<sup>-1</sup> is related with Y-O stretching [11]. The broad peaks at 3335 and 1647 cm<sup>-1</sup> is due to the -OH stretching and bending modes, which is from ethylene glycol used as capping agent during the synthesis of nanoparticles. When the as-prepared sample is annealed at 500 and 900°C, the -OH molecule present on the surface of the nanoparticles are decreases resulting decrease in intensity of O-H vibration is decreased. Another indication of ethylene glycol is stretching vibrations of -CH<sub>2</sub> groups present in ethylene glycol (EG) are observed distinctly at 2882 and 2957 cm<sup>-1</sup> [11].



Sl. No.	Samples Name	Lattice parameter (Å)		Crystallite sizes (nm)	Strain (%)
		a	c		
1	JCPDS No. 17-0341	7.119	6.289		
2	YVO <sub>4</sub> :2Dy, as-prepared	7.114	6.276	26	0.081
3	YVO <sub>4</sub> :2Dy, 500°C	7.110	6.297	25	0.049
4	YVO <sub>4</sub> :2Dy, 900°C	7.112	6.295	28	-0.122
6	YVO <sub>4</sub> :2Dy:2Ba, as-prepared	7.131	6.270	27	-0.201
7	YVO <sub>4</sub> :2Dy:2Ba, 500°C	7.120	6.310	21	-0.098
8	YVO <sub>4</sub> :2Dy:2Ba, 900°C	7.116	6.287	29	-0.074

**Table 1:** Lattice parameter and crystallite sizes of YVO<sub>4</sub>:2Dy and YVO<sub>4</sub>:2Dy:2Ba as-prepared and at different annealing temperature of 500 and 900°C.

### Transmission electron microscopy study

TEM image of YVO<sub>4</sub>:2Dy nanoparticles annealed at 500°C is shown in Figure 3A. The particles are spherical in shape; some of the particles are seen as agglomerated. Most of the particles sizes are in the range of 20-45 nm but maximum numbers of particles have their sizes in the range of 25 nm. From HRTEM shown in inset (Figure 3A the calculated

values of  $d = 1.57 \text{ \AA}$  which can be assigned to (004) plane. In the SAED pattern also we observed spots in the diffracted rings which indicate crystallinity of the prepared nanoparticles is shown in Figure 3B.

Interestingly, in case of TEM image of nanohybrids (Figure 3C) the spherical particles are connecting in chain via PEG, which is used as binding agent between YVO<sub>4</sub> and Fe<sub>3</sub>O<sub>4</sub> molecules well bind the YVO<sub>4</sub> and Fe<sub>3</sub>O<sub>4</sub> molecule when nanohybrids is formed. In case of HRTEM also, we observed two phases were present in nanohybrids one corresponding to YVO<sub>4</sub> (indicated by Y) and another Fe<sub>3</sub>O<sub>4</sub> (indicated by Fe). For YVO<sub>4</sub> phase the HRTEM gives the  $d = 4.69 \text{ \AA}$  corresponding to (101) plane and for Fe<sub>3</sub>O<sub>4</sub>  $d = 4.82 \text{ \AA}$  corresponding to (111) plane. In the SAED pattern (Figure 3D) we observe more number of rings and spots in case of nanohybrids because it contains both Fe<sub>3</sub>O<sub>4</sub> and YVO<sub>4</sub>. From the above discussion it is observed that PEG molecules play important role in nanohybrids formation.

Figure 4A shows the excitation spectra of 2 at.% of Dy doped YVO<sub>4</sub> (YVO<sub>4</sub>:2Dy) for as-prepared, 500 and 900°C annealed samples monitor with emission wavelength at 574 nm (<sup>4</sup>F<sub>15/2</sub> → <sup>6</sup>H<sub>13/2</sub> transition of Dy<sup>3+</sup> ion). Broad absorption/excitation peaks in 250-350 nm, which is related to V-O charge transfer band (CTB i.e. indirect) [12]. CTB is due to absorption of light when one electron from O<sup>2-</sup> is transferred to V<sup>5+</sup> and then it becomes V<sup>4+</sup>-O<sup>-</sup> [12]. There is a shift of peak from lower to higher wavelength on annealing as-prepared sample to 500 or 900°C. This is related to increase in covalency between V and O ions upon annealing. The electron densities around V site decreases when it starts interact with O through electron sharing. Expansion of unit cell volume gives rise to higher sharing of electrons between V and O (i.e.

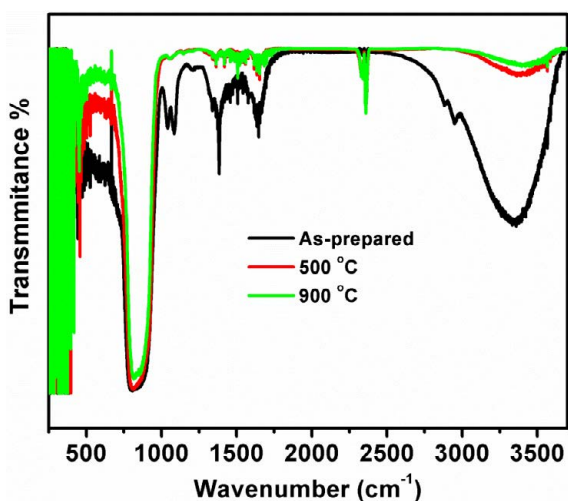


Figure 2: FTIR spectra of YVO<sub>4</sub>:2Dy as-prepared and annealed at different temperature 500 and 900°C.

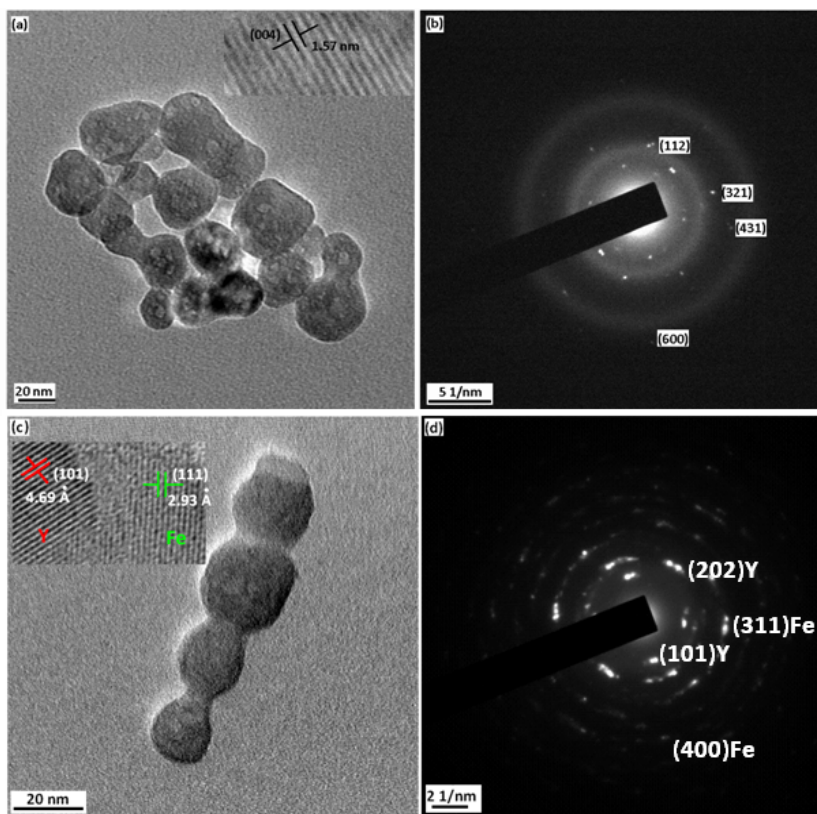


Figure 3: A) TEM image along with HRTEM (inset) and B) SAED pattern along with planes for YVO<sub>4</sub>:2Dy nanoparticles annealed at 500°C. C) TEM image of YVO<sub>4</sub>:2Dy/Fe<sub>3</sub>O<sub>4</sub> nanohybrids along with HRTEM (inset) and D) SAED patterns.

covalent bonding). Higher the covalent bonding more is the V-O CTB absorption is shifted to the higher wavelength. Also, there are sharp peaks in 350-500 nm, which are related to Dy<sup>3+</sup> absorption peaks (4f-4f transitions i.e. direct). The peaks at 355, 369, 393, 430, 456 and 476 nm are assigned to transitions of Dy<sup>3+</sup> from <sup>6</sup>H<sub>15/2</sub> to <sup>6</sup>P<sub>5/2</sub>, <sup>4</sup>K<sub>17/2</sub>, <sup>4</sup>I<sub>13/2</sub>, <sup>4</sup>G<sub>11/2</sub>, <sup>4</sup>I<sub>15/2</sub> and <sup>4</sup>F<sub>9/2</sub>, respectively [13]. Excitation at 320 nm gives the broad emission peak in 350-500 nm for pure YVO<sub>4</sub> sample [3]. The range 350-500 nm covers the absorption peaks of the Dy<sup>3+</sup> ion. Dy<sup>3+</sup> ion can absorb emitted photons from YVO<sub>4</sub> since absorption cross-section of VO<sub>4</sub><sup>3-</sup> of YVO<sub>4</sub> is high, number of the emitted photons is very high and these are simultaneously absorbed by Dy<sup>3+</sup> ions. Thus, it is expected that emitted photons from Dy<sup>3+</sup> (with VO<sub>4</sub><sup>3-</sup> host) will be much higher than Dy<sup>3+</sup> free ions, which is observed in emission study. Upon annealing the intensities of both V-O CTB and Dy<sup>3+</sup> increase due to decrease of non-radiative rate arising from H<sub>2</sub>O or defect present on the surface of particles [12-14].

Figure 4B shows the emission spectra of 2 at.% of Dy:YVO<sub>4</sub> excited at 320 and 355 nm. Normally, Dy<sup>3+</sup> ion shows the three emission bands in the visible range from the <sup>4</sup>F<sub>15/2</sub> level to the <sup>6</sup>H<sub>15/2</sub> (483 nm, magnetic dipole), <sup>6</sup>H<sub>13/2</sub> (574 nm, electric dipole) and <sup>6</sup>H<sub>11/2</sub> (655 nm) [13]. But in present case, peak at 655 nm is only seen in case of 320 nm excitation. Amongst them, peak at 574 nm has the highest intensity. The excitation through 320 nm (V-O CTB) gives the higher emission intensity than that of 355 nm. Since, at 320 nm excitation, extra photons emitted from VO<sub>4</sub><sup>3-</sup> transfer their energy to Dy<sup>3+</sup> ions indirectly. Thus, emitted photons from Dy<sup>3+</sup> are comparatively higher than its free ion Dy<sup>3+</sup> f-f transitions. On the other hand, on excitation at 355 nm, only few electrons are transferred to the excited state of Dy<sup>3+</sup> due to forbidden nature of f-f transitions. So, their emitted photon counts are low [15].

Figure 5A shows the emission spectra of the YVO<sub>4</sub>:2Dy nanoparticles, as-prepared and annealing at different temperature 500 and 900°C, respectively. Here, emissions spectra are monitored at V-O

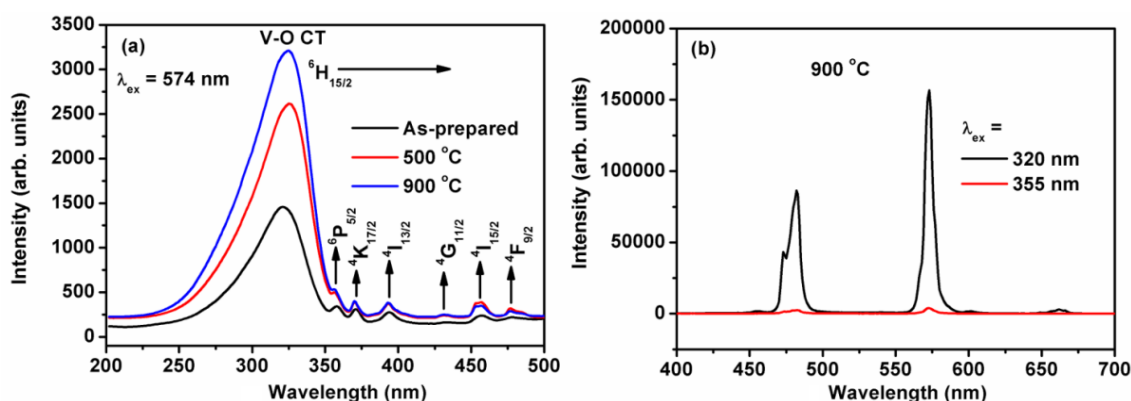


Figure 4: A) Excitation spectra of YVO<sub>4</sub>:2Dy monitored at 574 nm at different annealing temperature as-prepared, 500 and 900°C. B) Emission spectra of YVO<sub>4</sub>:2Dy monitored at two different excitations 320 and 355 nm for 900°C.

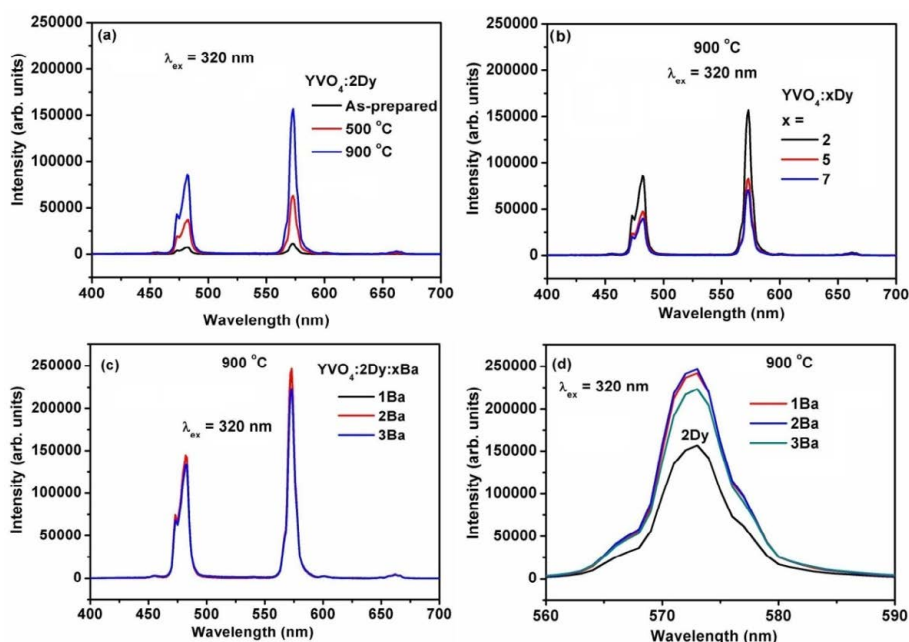


Figure 5: A) Emission spectra of YVO<sub>4</sub>:2Dy at different annealing temperature and B) Emission spectra of Dy doped YVO<sub>4</sub> nanoparticles at different concentration of Dy<sup>3+</sup> ion for 900°C. C) Emission spectra of Ba<sup>2+</sup>-codoped YVO<sub>4</sub>:2Dy at different concentration of Ba<sup>2+</sup> ion for 900°C and D) Comparison of emission spectra of YVO<sub>4</sub>:2Dy and Ba<sup>2+</sup> ion codoping at different concentration of Ba<sup>2+</sup> ion all the emission peaks are monitored at 320 nm excitation.

charge transfer band i.e. 320 nm. By exciting at V-O CTB we observed the emission peaks of Dy<sup>3+</sup> ion at 483 (strong), 574 (strongest) and 655 nm (small) which can be assigned as <sup>4</sup>F<sub>15/2</sub>-<sup>6</sup>H<sub>15/2</sub>, <sup>4</sup>F<sub>15/2</sub>-<sup>6</sup>H<sub>13/2</sub> and <sup>4</sup>F<sub>15/2</sub>-<sup>6</sup>H<sub>11/2</sub> of Dy<sup>3+</sup> ion [12,13]. There is strong energy transfer from host to dopant Dy<sup>3+</sup> ion (Scheme 1). The intensity of emission spectra increases with increase in annealing temperature also which is due to decreases of -OH/dangling bond present on the surface of the nanoparticles at higher annealing temperature [16].

Figure 5B shows the emission spectra of 900°C for annealed samples at different concentration of Dy<sup>3+</sup> ion 2, 5 and 7 at.%, respectively. The emission spectra show the typical emission of Dy<sup>3+</sup> ion at 483, 574 and 655 nm. The emission intensity of Dy<sup>3+</sup> ion decreases with increase in concentration of dopant ion. The intensity of the emission follows as 2>5>7 at.% of Dy<sup>3+</sup> ions. This can be explained as, when the concentration of Dy<sup>3+</sup> ion increase the distance between Dy<sup>3+</sup>-Dy<sup>3+</sup> ion pairs become lower and cross relaxation amongst the Dy<sup>3+</sup>-Dy<sup>3+</sup> ions increases [17].

Figure 5C shows the emission spectra of the Ba<sup>2+</sup> ion codoping YVO<sub>4</sub>:2Dy at 900°C annealed samples at their different codoping concentrations. There is no change in peak position of Dy<sup>3+</sup> ion emission with codoping although intensity of the dopant Dy is enhanced. From the Figure 5C we observed that the emission intensity is highest in case of 2 at.% Ba<sup>2+</sup> ion codoped YVO<sub>4</sub>:2Dy and lowest in case of 3 at.% codoped YVO<sub>4</sub>:2Dy nanoparticles. For more and clear understanding the enhancement of Dy<sup>3+</sup> ion we have shown expanded view in Figure 5D. The emission intensity follows the trend 2Dy<3Ba<1Ba<2Ba. From this, we concluded that optimum concentration of the Ba<sup>2+</sup> ion require for codoping in YVO<sub>4</sub>:2Dy is 2 at.%, above this concentration the intensity becomes decreases due to concentration quenching. The one of the reasons for enhancement of emission intensity of the YVO<sub>4</sub>:2Dy by Ba<sup>2+</sup> ion is due to increase of absorption coefficient. Such types of enhancement were reported in previous papers also [18,19]. They have reported that increase in absorption coefficient results in the enhancement of the emission intensity of lanthanide by Ba<sup>2+</sup> ion codoping. But, there is another important reason which is found here is that strain values are also play important role for enhancement of emission. From Table 1 we observed that the tensile strain value drop regularly with codoping with Ba<sup>2+</sup> ion. Decreasing tensile strain increase luminescence intensity i.e. intensity of YVO<sub>4</sub>:2Dy (500°C)>YVO<sub>4</sub>:2Dy (as-prepared) and within the compressive strain luminescence intensity increases with increasing compressive strain i.e. YVO<sub>4</sub>:2Dy:2Ba (900°C)>YVO<sub>4</sub>:2Dy:2Ba (500°C)>YVO<sub>4</sub>:2Dy (900°C)>YVO<sub>4</sub>:2Dy (as-prepared) [20]. In our case also, the tensile strain value of 2Dy

(-0.122%) is drop down to (-0.098%) in case of 2Ba and emission intensity of the Dy<sup>3+</sup> ion is being enhanced. The enhancement of emission intensity is also clearly seen from integrated area of the emission peak at 574 nm (Figure 6A and 6B) for 900°C annealed samples. The emission intensity of 2 at.% Ba<sup>2+</sup> ion codoped YVO<sub>4</sub>:2Dy nanoparticles is increased twice as that of without Ba<sup>2+</sup> ions.

Figure 7A-7D shows the decay curves for <sup>4</sup>F<sub>15/2</sub> level of Dy<sup>3+</sup> ion doped YVO<sub>4</sub> and Ba<sup>2+</sup> ion codoped nanoparticles annealed at 900°C for different concentration and different excitations 320 (indirect) and 355 nm (direct) wavelengths. Here, for all excitations the emission wavelength is fixed at 574 nm.

For indirect excitation (charge transfer transition) i.e. 320 nm we are using the non-linear curved fitted to data, Figure 7A and 7C. Here, we have included the study of relationship between diffusion and energy transfer mechanism for indirect excitations. The non-exponential equation is given below:

$$I_t = I_0 e^{\left(-\frac{x}{\tau_1} - Dx^{0.5}\right)}$$

Where D is related to diffusion and energy transfer. The detailed fitted result were summarised in Table 2. The lifetime value is well co-related with the emission intensities of various Ba<sup>2+</sup> ions concentrations. The lifetime values of 2Dy, 5Dy and 7Dy are 0.913, 0.874 and 0.846 ms, respectively. The corresponding rates constant are found as 1.095, 1.144 and 1.182 for 2Dy, 5Dy and 7Dy samples. Lifetime increase with increasing emission intensity of Dy<sup>3+</sup> ion. The lifetime value of 2Dy is longer than other two samples under same excitation which is due to higher intense emission of 2Dy than 5Dy and 7Dy samples. Same case is happening for other Ba<sup>2+</sup> codoping also, lifetime value of the 2Ba gives longest life time of 1.316 ms and its respective rate constant is 0.759.

In case of direct excitation (4f-4f transition) i.e. 355 nm the decay curve are well fitted by mono exponential. The equation used here is given as [17]

$$I_t = I_0 e^{-\frac{t}{\tau}}$$

Where  $I_t$  is intensity at time  $t$ , and  $I_0$  is intensity at  $t = 0$  and  $\tau$  is average lifetime. The lifetime value of direct excitation is shorter than the indirect excitations as shown in Table 2. This is related with the higher emission intensity of Dy<sup>3+</sup> ion in case of indirect due to energy transfer from VO<sub>4</sub> to Dy<sup>3+</sup> ion. Homogeneous distribution of dopant into host is indicated by monoexponential fitting [21].

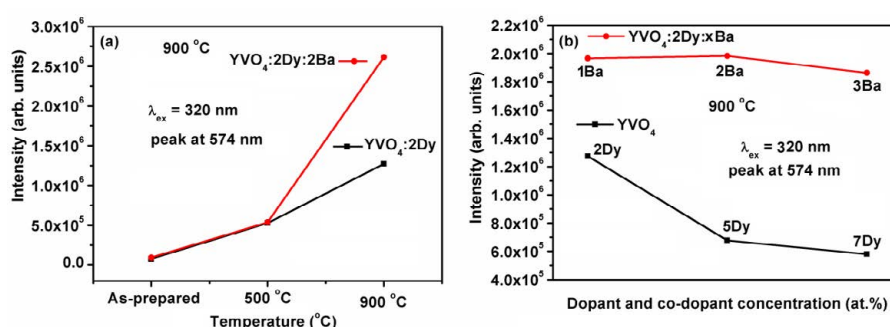
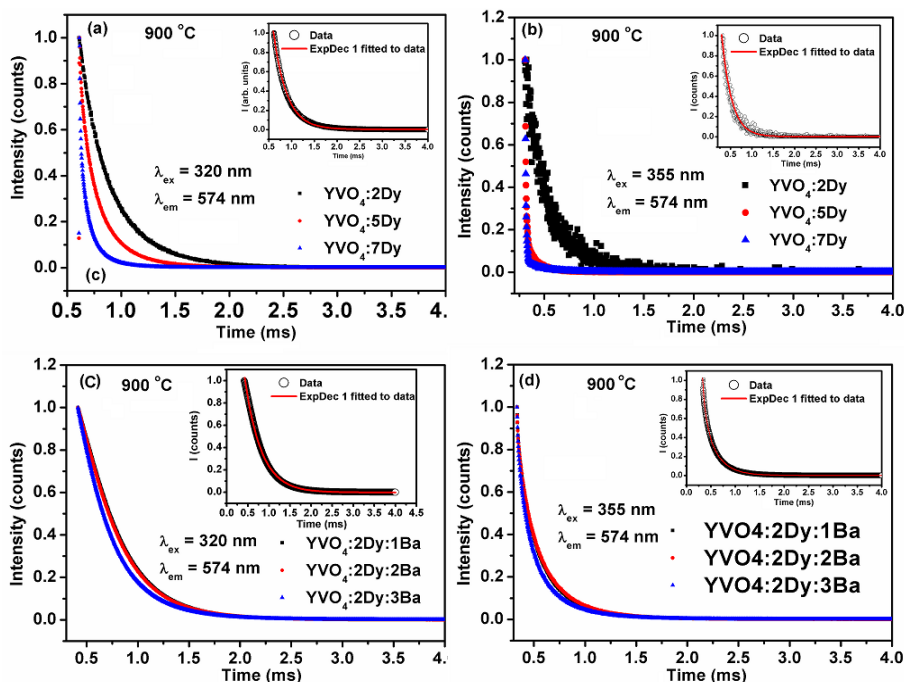


Figure 6: Integrated area of A) YVO<sub>4</sub>:2Dy and YVO<sub>4</sub>:2Dy:2Ba of the <sup>4</sup>F<sub>15/2</sub> to the <sup>6</sup>H<sub>13/2</sub> transition at different annealing temperature. B) Comparison of integrated area of YVO<sub>4</sub>:2Dy and YVO<sub>4</sub>:2Dy:2Ba for 900°C annealed samples for <sup>4</sup>F<sub>15/2</sub> to the <sup>6</sup>H<sub>13/2</sub> transition.



**Figure 7:** Decay curve of YVO<sub>4</sub>:2Dy at different excitation A) 320 nm and B) 355 nm. Decay curved of YVO<sub>4</sub>:2Dy:xBa at different excitation C) 320 nm and D) 355 nm. All the samples were annealed at 900°C.

Luminescence quantum efficiency ( $\eta$ ) is calculated from the total number of photons absorbed ( $\alpha$ ) and number of photons emitted ( $\epsilon$ ) from the sample as given below,

$$\eta = \frac{\epsilon}{\alpha} = \frac{\int I_{emission}}{\int I_{solvent} - \int I_{sample}}$$

Where  $I_{emission}$  is emission spectrum of sample,  $I_{solvent}$  is the intensity of absorbed light of solvent (methanol) and  $I_{sample}$  is the intensity of absorbed light for samples along with solvent together. difference between areas under curve of these two i.e.  $I_{solvent}$  and  $I_{sample}$  will give the corresponding total photons absorbed by sample. The quantum efficiencies calculated for nanoparticles annealed at 900°C are shown in Table 2. The quantum efficiency of YVO<sub>4</sub>:3Dy is found to be 29% and for 2 at.% Ba<sup>2+</sup> ion codoped YVO<sub>4</sub>:2Dy nanoparticles is 45%. The quantum efficiency of Ba<sup>2+</sup> ion codoping is higher than only Dy<sup>3+</sup> ion doped samples this is relate with intensity of the emission spectra.

### Hyperthermia study

In magnetic hyperthermia, there are four mechanisms which are mainly responsible for heat generation; Brownian rotation, Neel's relaxation, hysteresis loss and eddy current. Heat generation from eddy current is negligible compare to Brownian and Neel's which main component is for heat generation in the magnetic samples. The detailed studies of the heat generation during the hyperthermia had been reported elsewhere [8]. Heat generation from samples in terms of specific absorption rate (SAR) is given by the following relation.

The specific absorption rate (SAR) of the particles is given by

$$SAR = C \frac{\Delta T}{\Delta t} \frac{1}{m_{magn}}$$

Sl No.	Samples Name (900°C)	Lifetime (ms)		Quantum Yield (%)
		320 nm	355 nm	
		$y = I e^{-Dx^{0.5}}$	$y = I e^{-\frac{x}{\tau_1}}$	
1	YVO <sub>4</sub> :2Dy	$I_1=7.109$ $\tau_1=0.913$ ms $D=0.232$ $\chi^2=0.9997$	$\tau_1=3.746$ $\tau_1=0.225$ ms $\chi^2=0.9948$	29
2	YVO <sub>4</sub> :5Dy	$I_1=2.672$ $\tau_1=0.874$ ms $D=0.208$ $\chi^2=0.9989$	$I_1=6.944$ $\tau_1=0.187$ ms $\chi^2=0.9932$	21
3	YVO <sub>4</sub> :7Dy	$I_1=8.704$ $I_1=0.846$ ms $D=0.243$ $\chi^2=0.9949$	$I_1=4.875$ $\tau_1=0.184$ ms $\chi^2=0.9864$	15
4	YVO <sub>4</sub> :2Dy:1Ba	$I_1=53.39$ $\tau_1=1.316$ ms $D=0.645$ $\chi^2=0.9996$	$I_1=3.746$ $\tau_1=0.225$ ms $\chi^2=0.9948$	42
5	YVO <sub>4</sub> :2Dy:2Ba	$I_1=18.191$ $\tau_1=1.872$ ms $D=0.136$ $\chi^2=0.9973$	$\tau_1=3.664$ $\tau_1=0.238$ ms $\chi^2=0.9960$	47
6	YVO <sub>4</sub> :2Dy:3Ba	$I_1=22.166$ $\tau_1=1.055$ ms $D=0.487$ $\chi^2=0.9995$	$\tau_1=23.707$ $\tau_1=0.197$ ms $\chi^2=0.9914$	35

**Table 2:** Lifetime values of YVO<sub>4</sub>:2Dy, YVO<sub>4</sub>:5Dy, YVO<sub>4</sub>:7Dy, YVO<sub>4</sub>:2Dy:1Ba, YVO<sub>4</sub>:2Dy:2Ba and YVO<sub>4</sub>:2Dy:3Ba nanoparticles annealing at 900°C.

Where  $c$  is the specific heat capacity of sample. Usually, it is calculated from total weight of sample and water. Since the amount of sample compare to the amount of the water is negligible, specific heat capacity of water alone is comparable to total specific heat capacity. Therefore, its specific heat capacity of water which is  $4.18 \text{ J g}^{-1} \text{ K}^{-1}$  is used for calculations of heat generation.  $\Delta T/\Delta t$  can be found out from slope of the time dependent temperature curve.  $m_{\text{magn}}$  is the weight of Fe or Fe compound in the 1 mL of

Figure 8A shows the temperature scan attained by YVO<sub>4</sub>:2Dy/Fe<sub>3</sub>O<sub>4</sub> nanohybrids at various concentration 2, 4 and 6 mg of nanohybrids with applied AC current 400 A. In these whole ranges of concentrations, samples can achieve hyperthermia temperature (HT) 42°C within a short interval. Applying same current at 400 A, it is found that temperature attained is increased gradually with higher amount of Fe<sub>3</sub>O<sub>4</sub> contained (Figure 8A). HT achieved by 2 mg, 4 mg and 6 mg samples are 224, 82 and 70 second, respectively. The corresponding SAR values are 26, 75 and 93 W/g at constant current of 400A for 2, 4 and 6 mg of nanohybrids. When the concentration of the sample is fixed at 6 mg of nanohybrids with different AC current 200, 300 and 400 A, HT increased with increasing amount of applying current. HT cannot be achieved at 200 and 300 A AC current but soon it reaches 400 A AC current nanohybrids is started achieving HT (Figure 8B).

Figure 9A and 9B shows the excitation and emission spectra of nanohybrids. In the excitation spectrum, there is a strong peak at 300 nm and other peaks originated from Dy<sup>3+</sup> ion are canvassed by this strong peak. Unlikely with excitation spectra of YVO<sub>4</sub>:2Dy which

has the highest intensity peak at 320 nm (V-O CT); the hybrid shows the strongest peak at 300 nm which is assigned to exciton formation between YVO<sub>4</sub>:2Dy and Fe<sub>3</sub>O<sub>4</sub> interface. Such type of exciton formation was reported in some previous papers [8,22]. Here, we strongly believe that the peak normally observed at 320 nm is being canvassed by the strong exciton peak at 300 nm since after the formation of hybrid it is confirmed that both emission and excitation are lower than corresponding values of YVO<sub>4</sub>:2Dy but after the formation of hybrid peak at 300 nm is still remained as a strong peak from which it is concluded that it is generated from exciton. In the emission spectra (Figure 9B) we observed the characteristics peaks of Dy<sup>3+</sup> ion at 483 and 574 nm. The peak at 574 nm lies in the biological window which means that the prepared nanohybrid can be used for the purpose of bioimaging too.

### Toxicology analysis

To study cytotoxicity of the prepared nanohybrids we performed the percentage viability test in HeLa cells (Figure 10) with variable concentrations of nanohybrids. Different samples containing 10, 20, 40, 80, 100 µg/L of nanohybrids has viability 98, 97, 96, 94 and 92, respectively. As we seen in Figure 10 viability percentage drops with increase in amount of nanohybrid. Here PEG-600 solution (100 mg/100 mL) is used as medium or control. This experiment shows that the prepared nanohybrid was found to have high viability.

Figure 11A and 11B shows the digital images for both control and YVO<sub>4</sub>:2Dy/Fe<sub>3</sub>O<sub>4</sub> nanohybrid after treatment with HeLa cell, at 100

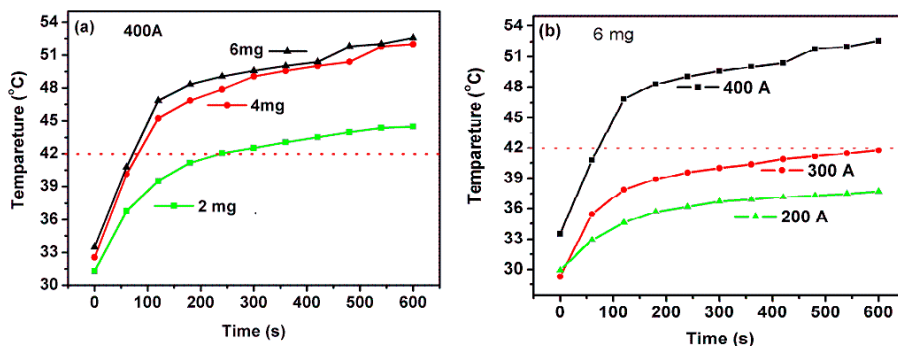


Figure 8: A) Temperature attained by YVO<sub>4</sub>:2Dy/Fe<sub>3</sub>O<sub>4</sub> nanohybrids at different concentration of nanohybrids at 400 A. B) Temperature achieved by YVO<sub>4</sub>:2Dy/Fe<sub>3</sub>O<sub>4</sub> nanohybrids at different values of current with fixed nanohybrids concentration (6 mg).

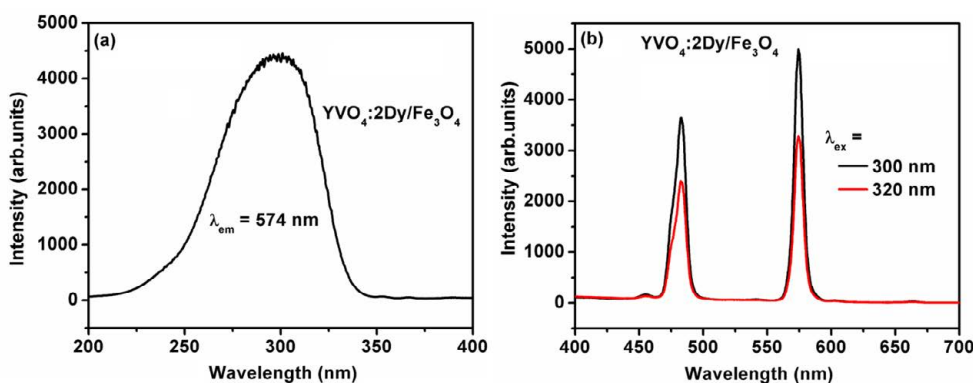
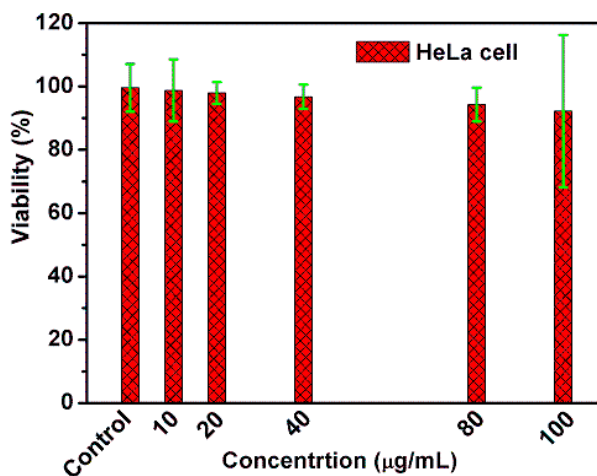
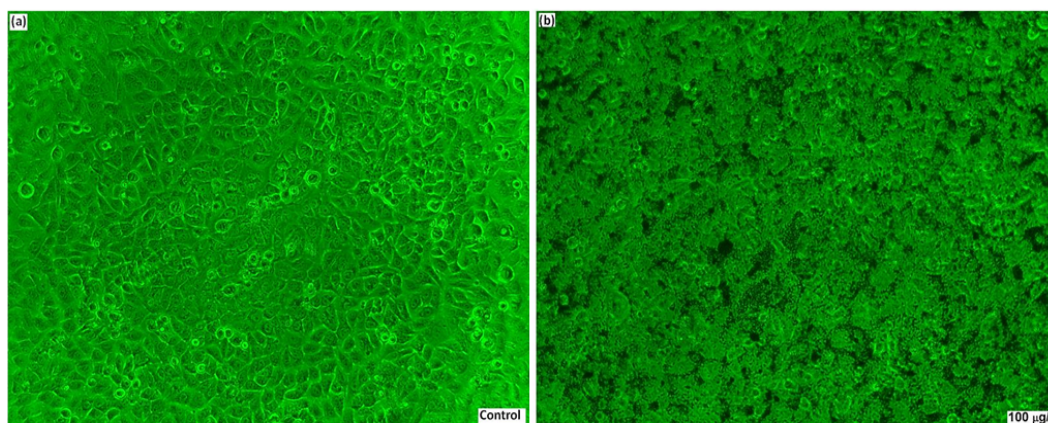


Figure 9: A) Excitation spectrum of YVO<sub>4</sub>:2Dy/Fe<sub>3</sub>O<sub>4</sub> nanohybrid monitored at 574 nm emission wavelength. B) Emission spectra of YVO<sub>4</sub>:2Dy/Fe<sub>3</sub>O<sub>4</sub> nanohybrid monitored at two different excitation wavelength 300 and 320 nm.



**Figure 10:** The percentage viability of HeLa cells treated with PEG solution (control) and YVO<sub>4</sub>:2Dy/Fe<sub>3</sub>O<sub>4</sub> nanohybrid at different concentrations. PEG solution is prepared by dissolving 100 mg of PEG-6000 in 100 mL of distilled water. Nanoparticles are dispersed in 1 mL of PEG solution.



**Figure 11:** Digital photograph showing before and after treatment with YVO<sub>4</sub>:2Dy@Fe<sub>3</sub>O<sub>4</sub> nanohybrid (A) control (without nanohybrid) and (B) YVO<sub>4</sub>:2Dy@Fe<sub>3</sub>O<sub>4</sub> nanohybrid at 100 µg/L concentration.

µg/L of nanohybrid. We observed that the nanohybrid is distributed homogeneously within HeLa cell instead of confining at a particular cellular region. Thus, this nanohybrid can be used for biological leveling for treatment of cancer cells as this nanohybrids already gives good results in hyperthermia application.

## Conclusion

In summary, spherical shape of Dy<sup>3+</sup> ion doped YVO<sub>4</sub> nanoparticles were prepared at different concentration of Dy<sup>3+</sup> and study its luminescence properties at different annealing temperature at 500 and 900°C. The role of PEG molecule which is use as binding agent in YVO<sub>4</sub>:2Dy/Fe<sub>3</sub>O<sub>4</sub> nanohybrid formation can easily be seen from TEM image of nanohybrid. The enhancement of the luminescence intensity after Ba<sup>2+</sup> ions codoping is also studied and optimum concentration of Ba<sup>2+</sup>codopant is found to be 2 at.%. Enhancement of emission intensity with codoping is due to increase in absorption coefficient and decrease in lattice strain values. Energy transfer is also studied from the decay data and its relation with diffusion and energy transfer for indirect excitation also studied. It can achieved quantum efficiency up to 45% for 2 at.% Ba<sup>2+</sup> ion codoping in YVO<sub>4</sub>:2Dy nanoparticles. YVO<sub>4</sub>:2Dy/Fe<sub>3</sub>O<sub>4</sub> nanohybrids are prepared to study its hyperthermia applications. It can achieved

hyperthermia temperature 42°C in very short period and viability up to 94% in HeLa cancer cells which makes them a good candidate for cancer treatment applications. The nanohybrid shows good luminescence in biological windows indicating that the prepared nanohybrids can be used for and bio-imaging purposed also.

## Acknowledgements

LaishramPriyobarta Singh thanks the DST national post-doctoral fellowship (PDF/2016/000370) for providing fellowship during research. NingthoujamPremananda Singh thanks the Council of Scientific and Industrial Research (CSIR), New Delhi, for the Senior Research Fellowship.

## References

1. Shahi PK, Singh P, Singh AK, Singh SK, Rai SB, et al. (2016) A strategy to achieve efficient dual-mode luminescence in lanthanide-based magnetic hybrid nanostructure and its demonstration for the detection of latent fingerprints. J Colloid Interface Sci 49: 199-206.
2. Jeyaraman J, Shukla A, Sivakumar S (2016) Targeted stealth polymer capsules encapsulating Ln<sup>3+</sup>-doped LaVO<sub>4</sub> nanoparticles for bioimaging applications. ACS Biomater Sci Eng 2: 1330-1340.
3. Singh LP, Jadav, NV, Sharma S, Pandey BN, Srivastava SK, et al. (2015) Hybrid nanomaterials YVO<sub>4</sub>:Eu/Fe<sub>3</sub>O<sub>4</sub> for optical imaging and hyperthermia in cancer cell. J Mater Chem C 3: 1965-1975.

4. Kaczmarek, AM, Ndagsi D, Deun RK (2016) Dopant and excitation wavelength dependent color tunability in Dy<sup>3+</sup>:YVO<sub>4</sub> and Dy<sup>3+</sup>/Eu<sup>3+</sup>:YVO<sub>4</sub> microparticles towards white light emission. *Dalton Trans.* 4: 6231-16239.
5. Ropp RC (1968) Spectra of some rare earth vanadates. *J Electrochem Soc* 115: 940-945.
6. Xie L, Song H, Wang Y, Xu W, Bai X, et al. (2010) Influence of concentration effect and Au coating on photoluminescence properties of YVO<sub>4</sub>:Eu<sup>3+</sup> nanoparticles colloids. *J Phys Chem C* 114: 9975-9980.
7. Ningthoujam RS, Rai SB, Dwivedi Y (2012) Nova Science Publishers Inc., Hauppauge, USA.
8. Singh LP, Ningthoujam RS, Srivastava SK, Mishra R (2014) Multifunctional hybrid nanomaterials from water dispersible CaF<sub>2</sub>:Eu<sup>3+</sup>,Mn<sup>2+</sup> and Fe<sub>3</sub>O<sub>4</sub> for luminescence and hyperthermia application. *J Phys Chem C* 118: 18087-18096.
9. Ghosh R, Pradhan L, Yensenbam PD, Meena SS, Tewari R, et al. (2011) Induction heating studies of Fe<sub>3</sub>O<sub>4</sub> magnetic nanoparticles capped with oleic acid and polyethylene glycol for hyperthermia. *J Mater Chem* 21: 13388-13398.
10. Williamson GK, Hall WH (1953) X-ray line broadening from fcc aluminium and olfram. *Acta metall* 1: 22-31.
11. William K (1987) *Organic Spectroscopy* Macmillan Educational Ltd., Houldmills, Hampshire.
12. Luwang MN, Ningthoujam RS, Srivastava SK, Vasta RK (2011) Preparation of white light emitting YVO<sub>4</sub>:Ln<sup>3+</sup> and silica coated YVO<sub>4</sub>:Ln<sup>3+</sup> (Ln<sup>3+</sup>=Eu<sup>3+</sup>, Dy<sup>3+</sup>, Tm<sup>3+</sup>) nanoparticles by CTAB/n-butanol/haxane/water microemulsion route: energy transfer and site symmetry studies. *J Mater Chem* 21: 5326-5337.
13. Li J, Li JG, Liu S, Li X, Sun X, et al. (2013) Greatly enhanced Dy<sup>3+</sup> emission via efficient energy transfer in gadolinium aluminate garnet (Gd<sub>3</sub>Al<sub>5</sub>O<sub>12</sub>) stabilized with Lu<sup>3+</sup>. *J Mater Chem C* 1: 7614-7622.
14. Ningthoujam RS, Singh LR, Sudarsana V, Singh SD (2009) Energy transfer process and optimum emission studies in luminescence of core-shell nanoparticles: YVO<sub>4</sub>:Eu-YVO<sub>4</sub> and surface state analysis. *J Alloy Comp* 484: 782-789.
15. Blasse G, Grabmaier BC (1994) *Luminescent Materials*; Springer-Verlag: Berlin.
16. Singh LP, Luwang MN, Srivastava SK (2014) Luminescence and photocatalytic studies of Sm<sup>3+</sup> ion doped SnO<sub>2</sub> nanoparticles. *New J Chem* 38: 115-121.
17. Singh NS, Ningthoujam RS, Yaiphaba N, Singh SD, Vasta RK (2009) Lifetime and quantum yield studies of Dy<sup>3+</sup> doped GdVO<sub>4</sub> nanoparticles: Concentration and annealing effect. *J Appl Phys* 105: 064303-1-7.
18. Tian L, Mho S (2007) Enhanced photoluminescence of YVO<sub>4</sub>:Eu<sup>3+</sup> by codoping the Sr<sup>2+</sup>, Ba<sup>2+</sup> or Pb<sup>2+</sup> ion. *J Lumin* 122: 99-103.
19. Wang G, Kim R, Qin W, Zhang D, Wang L, et al. (2008) Enhanced photoluminescence of water soluble YVO<sub>4</sub>:Ln<sup>3+</sup> (Ln=Eu, Dy, Sm, and Ce) nanocrystals by Ba<sup>2+</sup> Doping. *J Phys Chem C* 112: 17042-17045.
20. Aumer ME, LeBoeuf SF, Bedair SM, Lin JY, Jiang HX (2000) Effects of tensile and compressive strain on the luminescence properties of AlInGaN/InGaN quantum well structures. *Appl Phys Lett* 77: 821-823.
21. Sivakumar S, Veggel FC, Raudsep M (2005) Bright white light through up-conversion of a single NIR source from Sol-Gel-derived thin film made with Ln<sup>3+</sup>-doped LaF<sub>3</sub> nanoparticles. *J Am Chem Soc* 127: 12464-12465.
22. Ningthoujam RS (2010) Generation of exciton in two semiconductors interface:SnO<sub>2</sub>:Eu-Y<sub>2</sub>O<sub>3</sub>. *Chem Phys Lett* 497: 208-212.